# Flaw Tolerance in Lap Shear Brazed Joints — Part 1

*Investigation brings a better understanding of the failure mechanism in brazed joints containing defects*

BY Y. FLOM AND L. WANG

ABSTRACT. Furnace brazing is a joining process used in the aerospace and other industries to produce strong permanent and hermetic structural joints. As in any joining process, brazed joints have various imperfections and defects. At the present time, our understanding of the influence of the internal defects on the strength of the brazed joints is not adequate. The goal of this three-part investigation is to better understand the properties and failure mechanisms of the brazed joints containing defects. This study focuses on the behavior of brazed lap shear joints because of their importance in manufacturing aerospace structures. In Part 1, an average shear strength capability and failure modes of the single lap joints are explored. Stainless steel specimens brazed with pure silver are tested in accordance with the AWS C3.2 standard. Comparison of the failure loads and the ultimate shear strength with the finite element analysis (FEA) of the same specimens as a function of the overlap widths shows excellent correlation between the experimental and calculated values for the defect-free lap joints. A damage zone criterion is shown to work quite well in understanding the failure of the braze joints. In Part 2, the findings of Part 1 will be verified on the larger test specimens. Also, various flaws will be introduced in the test specimens to simulate incomplete braze coverage in the lap joints. Mechanical testing and FEA will be performed on these joints to verify that behavior of the flawed ductile lap joints is similar to joints with a reduced braze area. Finally, in Part 3, the results obtained in Parts 1 and 2 will be applied to the actual brazed structure to evaluate the load-carrying capability of a structural lap joint containing discontinuities. In addition, a simplified engineering procedure will be offered for the laboratory testing of the lap shear specimens.

*Y. FLOM is with NASA Goddard Space Flight Center, Greenbelt, Md. L. WANG is with SWALES Aerospace, Beltsville, Md.*

## Introduction

In manufacturing of critical brazements, one of the main variables controlling the strength of the lap shear braze joints is the width of the braze overlap. By allowing sufficient overlap width, the strength of the braze joint (i.e., the load-carrying capability) can be made equal to or even greater than the strength of the base metal. At the same time it is now well established that the average maximum shear stress of the lap joint at the failure load decreases with the increase of the overlap width (Ref. 1), as shown in Fig. 1. The presence of the defects, however, can compromise the integrity of the braze joints. Modern nondestructive inspection methods help to identify and weed out the defective joints. In some cases, however, a structure or a pressure vessel containing defective braze joints is too expensive to be scrapped. Therefore, it is beneficial to understand how the defects affect the performance of the braze joints so the best engineering decisions could be made to ascertain the acceptability of the brazed structure. An attempt by the authors to find any references in open literature that examine the load-carrying capability of braze joints in the presence of internal discontinuities was not very successful. A lack of research publications studying the effects of discontinuities on the properties of the brazed joints is somewhat puzzling. It is particularly so considering that the issues of stress distribution, load-carrying capability, damage tolerance, and failure mechanisms in structural bonded joints had received a great deal of attention in the research community (Refs. 2–4). For example, a theoretical analysis of stresses in adhesive lap joints had been presented as early as 1938 (Ref. 5). Just the fact that there are at least 13 ASTM standards developed to perform shear tests on various adhesive-bonded test specimens indicates a much higher level of effort devoted to understanding the properties of structural-bonded joints.

KEY WORDS

Aerospace
Brazement
Brazing
Furnace Brazing
Lap Joints

A number of industrial and government quality control standards address the acceptable limits for internal discontinuities in brazed joints (Refs. 6–12). The acceptance criteria are based either on the maximum aggregate braze area reduction due to the voids, inclusions, or incomplete braze (up to 15–20% of the total area of the joint) or reduction of the leakage barrier width. Some documents allow up to 15% reduction of the leakage barrier (Ref. 7), but other ones permit the width of the largest void or unbonded region to be up to 60% of the total joint width (Refs. 8–10). Military specification MIL-B-007883C provided a more extensive treatment of the internal discontinuities, but it has been cancelled. In addition, the guidelines provided by this specification for accepting or rejecting internal defects were not very clear.

The authors could not find any reference in open literature addressing the strength of the structural braze lap joints containing internal discontinuities. Obviously, the criteria based on percentage reduction of the aggregate braze area do not apply to long joints. One can be well below the maximum allowable area reduction, and, therefore, be within the "acceptable" limits but have all the flaws concentrated in a relatively short section of the seam causing the entire lap joint to fail locally — Fig. 2.

This study focuses on lap shear joints due to their importance in the manufacturing of large brazed pressure vessels. The following questions will be addressed:

1) What is the criterion of failure for a lap shear braze joint?

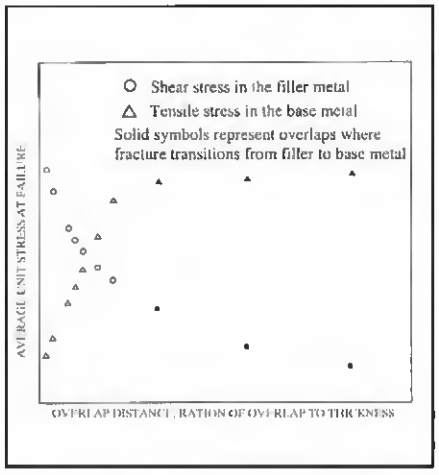


*Fig. 1 — A general representation of the maximum average shear stress in the filler metal as well as the tensile stress in the base metal as a function of the overlap width in the braze joint. This graph is based on the hundreds of tests performed in the early 1960s (Ref. 1) and many subsequent experimental results reported in literature.*

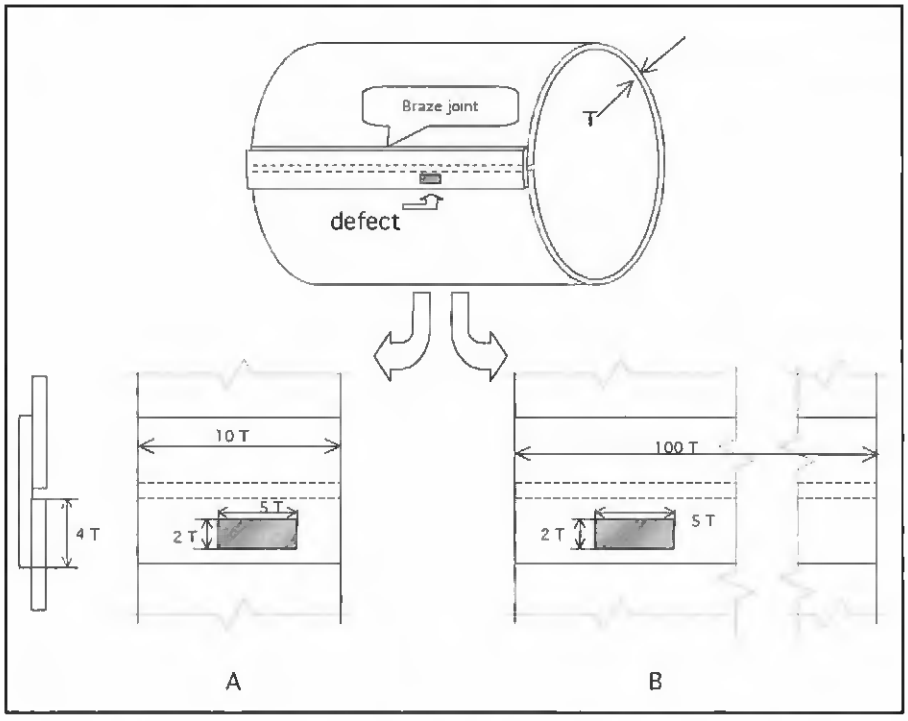


*Fig. 2 — Illustrates inconsistency in using maximum allowable area reduction approach. Consider two different situations of brazing 10T long and 100T long pressure vessel. Assume, for example, that in both cases the braze joint has a flaw (shaded area) and its size is 2T × 5T. In one case (A), the ratio of the flaw area to the total braze area is 10/40, i.e., 25%. In case B, the ratio is 10/400 or only 2.5%. If we apply 15% maximum allowable braze area reduction rule then the joint will be rejected in case A and accepted in case B.*

2) Can the effect of internal discontinuities on the strength of ductile lap joints be viewed simply as a reduction of the actual load-bearing area?

3) How do we determine load-carrying capacity of braze lap joints containing internal defects?

4) Is there a maximum flaw size that can cause a transition from ductile to brittle failure in a lap joint?

The objectives of the Part 1 effort were as follows:

- Perform strength measurements of the lap shear brazed joints as a function of overlap width per AWS C3.2 (Ref. 12).
- Perform finite element analysis (FEA) of the test specimens.
- Develop failure criterion
- Correlate FEA with the experimental data.

## Experimental Procedures

In this study, 347 stainless steel (see Table 1 for composition) test specimens were vacuum brazed using 99.9% pure silver filler metal. These materials were selected for their important role in the aerospace industry. Using a single-phase filler metal helps to eliminate possible influence of the eutectic or multiphase microstuctures on the results of this investigation.

A single lap shear test specimen (STS) configuration and fabrication was based on the AWS C3.2 specification, with some deviations due to material availability and fabrication cost. It is believed, however, that these differences did not compromise the objectives set forth in the present work.

The "half of the dog bone" shaped blanks were electric discharged machined from a 0.090-in. (2.3-mm) -thick stainless steel strip and plated with a 0.0005-in. (0.0127-mm) -thick layer of Ni prior to brazing in order to facilitate wetting of the base metal. The majority of the shear test specimens (STS) were Ni plated using electroless process. Several of the STS were electrolytically Ni plated to eliminate the presence of low-melting Ni-P eutectic. All blanks were assembled for brazing in the specially designed stainless steel fixture — Fig. 3. Silver filler metal in the form of the 0.0010-in. (0.254-mm) foil was preplaced in the overlap. A pair of blanks form one complete "dog bone" shaped STS. The top blank was allowed to float in such a way that it could move down under its own gravity and along the longitudinal axis of symmetry during brazing while maintaining an axial alignment with the bottom blank. Consequently, the braze joint clearance was not rigidly controlled but rather was allowed to form on its own under the combined action of the blank weight and the capillary forces of the molten filler. This freedom of movement assured that the braze joint clearance and the alignment of the test specimens were not affected by the differences in thermal properties between the fixture and the specimens. Each STS was brazed one at a time in the vacuum brazing furnace using the identical brazing cycle. The maximum brazing temperature was 1020°C. The overlap width was adjusted manually for each pair of blanks to cover the range 0.05T to 5T, which corresponds to 0.045 in. (1.14 mm) and 0.450 in. (11.4 mm), where T= 0.090 in. (2.3 mm) is the base metal thickness. Since the blanks were not clamped during brazing and the faying interfaces were allowed to move relative to each other, the overlap widths on the brazed specimen were slightly different from the preset values due to variations in the coefficients of thermal expansion of the specimens and various components of

*Fig. 3 — Shear test specimen blanks assembled for brazing.*

Table 1 — Composition of 347 Stainless Steel (%)

| C | Mn | P | S | Si | Cr | Ni | Nb/Ta | Fe |
|---|---|---|---|---|---|---|---|---|
| 0.08 | 2 | <0.05 | <0.03 | 1 | 17–19 | 9–13 | 0.62 | balance |

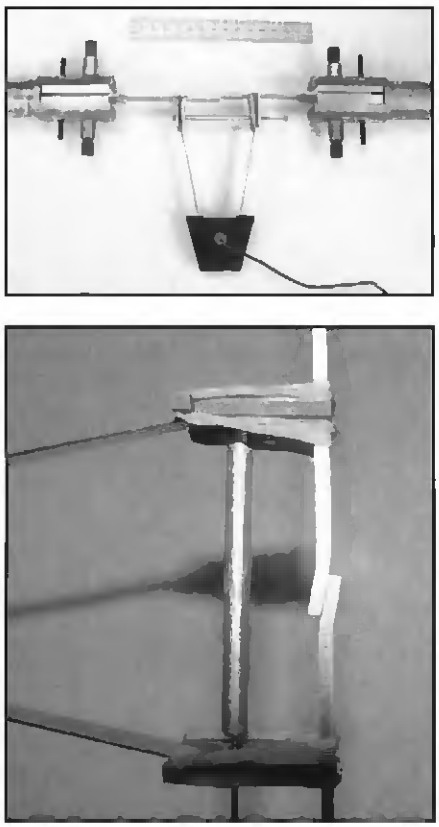

*Fig. 4 — Extensometer installed on the shear specimen prior to test shown on the top. Picture on the bottom shows the gauge length portion of the test specimen under the load.*

the brazing fixture. Fillets were removed from each end of the STS with the specially ground end mill bit to maintain the same fillet radius of 0.016 in. (0.4 mm) on all specimens.

A total of 37 lap shear specimens were tensile tested to failure. A 2-in. (50.8-mm) gauge length extensometer was used to measure elongation of each test specimen — Fig. 4. The extensometer arms used different length knife edges to compensate for the 1T offset in the geometry of the single lap shear specimen. As a result, the influence of the test specimen rotation on the elongation measurements was minimized at least during the initial portion of the tensile test. Each test was videotaped to ensure that the deformation behavior of the lap shear specimens, dynamics of fracture process, and other important features were captured.

### Finite Element Analysis

Finite element analyses (FEA) were performed using COSMOS/M package. Plane strain nonlinear elasto-plastic elements were used throughout the analysis. A typical model with parametric meshing is shown in Fig. 5. The total length of the model is kept at 2 in. (50.8 mm). This is consistent with the extensometer gauge length including the lap width. A perfect bond is assumed between the filler metal and the base metal. The true stress strain curve of the 347 stainless steel was established by tensile testing of the material. The true stress strain curve of the filler metal (annealed pure silver) was based on tensile testing of the material and the data obtained from private communications (Ref. 13). The final form of the true stress strain curves is shown in Fig. 6. Both curves are averages of at least three repetitive test results. The loading process of the FEA model is accomplished by incrementally applying a uniform displacement at one end of the specimen while keeping the other end fixed in the loading direction. The overall tensile load applied to the specimen at each loading step is the integration of the tensile stress in the loading direction of the end elements. In average, about one hundred loading steps were used to complete a loading process. Instead of nodal, the elemental stresses/strains were used to describe the stress/strain level within the filler metal since it is relatively thin and experiences large plastic deformation.

## Experimental Results

Typical cross sections of the 347/Ag/347 braze joints are shown in Fig. 7. As expected, the microstructure of the filler metal is a single phase consisting of pure silver. The interface regions vary, however, depending on whether the electrolytic or electroless process was used for Ni plating. In the case of electroless Ni, the brazed interfaces contain small inclusions of $Ni_3P$ compound since the brazing temperature exceeded the nickel-phosphorus eutectic point of 880°C.

Typical load vs. elongation records for the tested specimens are shown on one plot in Fig. 8. As was mentioned earlier, the actual overlap lengths in the lap shear STS varied, slightly, from the exact multiples of 0.5T. Consequently, it was more convenient to group the individual records into the 0.5T intervals, as shown in Fig. 8. All test specimens failed in the filler metal. During the initial part of the tension test, the braze joints rotated to reduce the loading axial offset between the top and the bottom ends of the test specimens. After the alignment was achieved, no further rotation was observed. The specimens continued to deform by uniform stretching of the base metal away from the joint. When the failure load was reached, the braze joint just slipped apart to cause the applied load to drop. No apparent peeling of the joint edges at the moment of failure was observed.

The maximum load in every test was defined as the failure load for that specific overlap. A plot of the failure load as a function of the overlap width is shown in Fig. 9A. Maximum average or apparent failure shear strength for each overlap width was calculated as the failure load divided by the area (overlap width × width of the specimen). Despite the fact that this value changes with the overlap width, it is beneficial to call it shear ultimate strength (SUS) of the lap shear braze joint in order to be consistent with the engineering terminology widely used within the structural design community. Hence, from now on, the term SUS will be used throughout this three-part investigation. A plot of the SUS as a function of overlap width is shown in Fig. 9B. A close examination of the data plotted in Fig. 9 shows that the data points seem to follow two different paths of strength values when the overlaps exceed

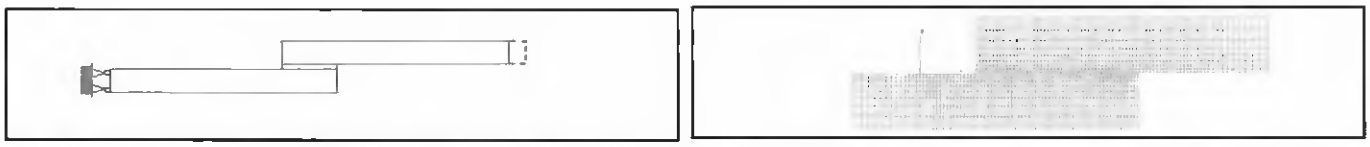

*Fig. 5 — COSMOS/M finite element analysis (FEA) 2-D model used in this investigation showing displacement boundary condition (left) and a typical FEA mesh (right).*

2T. The higher strength path corresponds to electrolytic Ni-plated specimens and the lower strength path to the electroless plated ones.

### FEA Results

The FEA exhibits satisfactory results in simulation of the loading process. A typical result of the deformed specimen model is shown in Fig. 10. A step-by-step examination of model deformation process also revealed that the lap joint rotates at the beginning of the loading process, as described earlier, followed by uniform stretching of the base metal as the loading axial offset diminishes. A FEA animation of the loading process vividly reproduced the tensile test as recorded on the tape.

## Discussion

As the mechanical testing demonstrated, for overlaps over 2T, the electrolytically plated braze joints are stronger than the electroless plated ones, as shown in Fig. 9. Consequently, for the purpose of this investigation, only high-strength values, obtained on the electrolytically plated test specimens, will be considered for correlation with the FEA results, since FEA does not account for the presence of $Ni_3P$ inclusions at the braze interface.

It is well established that plastic deformation of the lap joints loaded in tension is controlled by the shear and peel (i.e., tensile load acting perpendicular to the interface) forces. Indeed, high magnification images of the fracture surfaces shown in Fig. 11 clearly indicate the existence of at least two distinct deformation regions within the braze joint. Fracture initiation region located at the lap edge is a combination of shear and peel, whereas the rest of the fracture area is dominated by pure shear. No evidence of peel was observed on the fracture surfaces of the specimens with overlaps < 2T.

While analyzing the deformation of the brazed joints, it is instructive to discuss our understanding of what constitutes a failure of the flaw-free lap shear braze joint. In this study we are assuming that the yielding of the braze joint does not constitute its failure. This assumption is based on the fact that some brazed structures such as rocket engines, for example, are designed to perform beyond their yield point. Thus, in the context of our study we define the failure as an event of fracture when the joint loses its load-carrying capability due to physical separation through the filler metal, base metal, or combination of the two.

Since most of the stress-strain properties of metals and alloys were obtained in tensile tests, the von Mises stress and yield criterion was used in the finite element analysis, even though the filler metal in the lap shear joint is almost in the pure shear condition. Tresca yield criterion may give a better prediction of the yielding of the filler metal. But due to the fact that the filler metal experiences a large amount of plastic deformation before failure, the onset of the yielding is less important in the current investigation. In addition, the von Mises stress, that is the effective stress in plasticity, is also the choice of the COSMOS/M package to handle plasticity. The von Mises stress is defined as (Ref. 14)

$$\sigma_{vm} = \frac{1}{\sqrt{2}} \times \sqrt{\left(\sigma_1 - \sigma_2\right)^2 + \left(\sigma_2 - \sigma_3\right)^2 + \left(\sigma_1 - \sigma_3\right)^2} \quad (1)$$

where $\sigma_1$, $\sigma_2$, and $\sigma_3$ are principal tensile stresses. In the current investigation, all

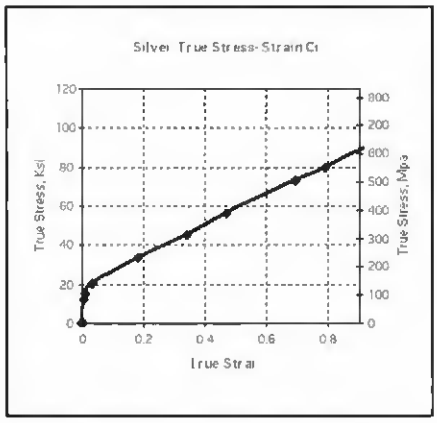


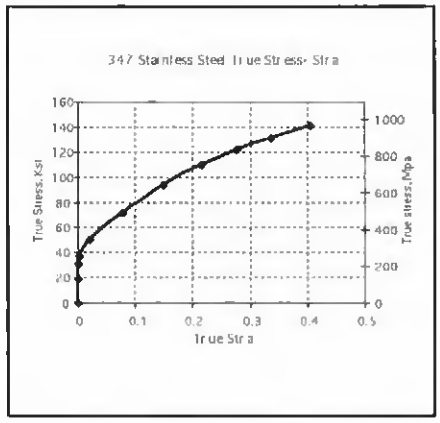


*Fig. 6 — True stress-strain curves for 347 stainless steel base metal and pure silver filler metal used in this work.*

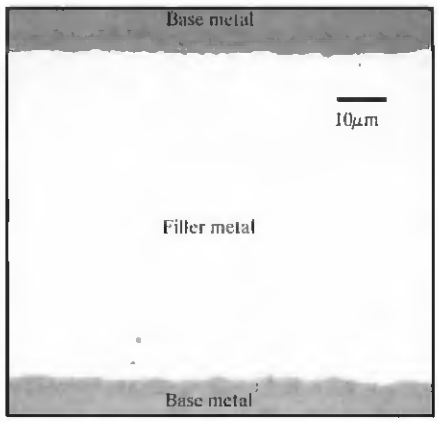


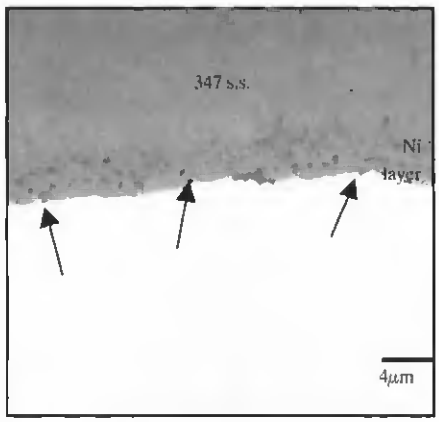


*Fig. 7 — Metallographic cross section through the braze joint. Image on the left captures the entire joint clearance width and shows basically single-phase silver filler metal. Image on the right is a higher magnification of the interface region showing a presence of small $Ni_3P$ inclusions (arrows). Also, a Ni layer can be seen separating the stainless steel base metal and silver filler metal.*

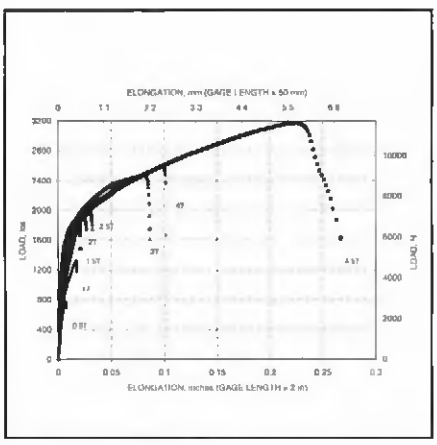

*Fig. 8 — Typical load vs. elongation plots representing overlaps ranging from 0.5T to 4.5T. Most likely, the three different slopes visible for all families of curves correspond to elastic, plastic rotation, and plastic stretching portions of the shear test specimen deformation during the pull test.*

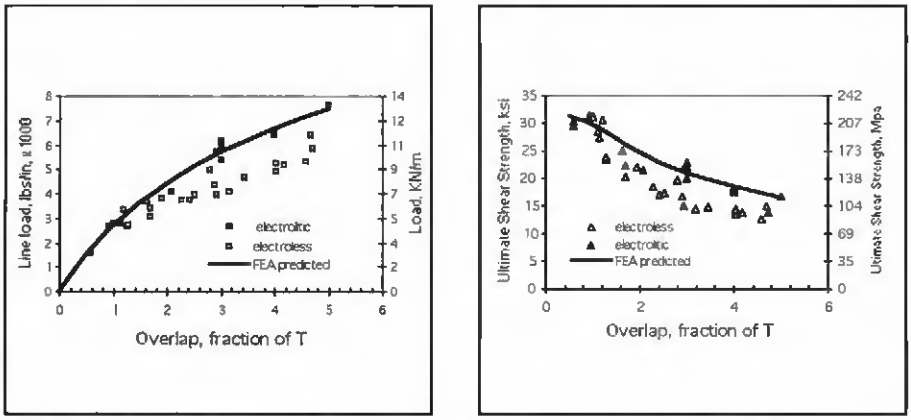


*Fig. 9 — Maximum load (A) and maximum average or stress shear ultimate strength (B) plotted as a function of the overlap size. Also shown are the FEA curves predicting similar values. As one can see electrolytically plated specimens show a better fit with the FEA curves.*

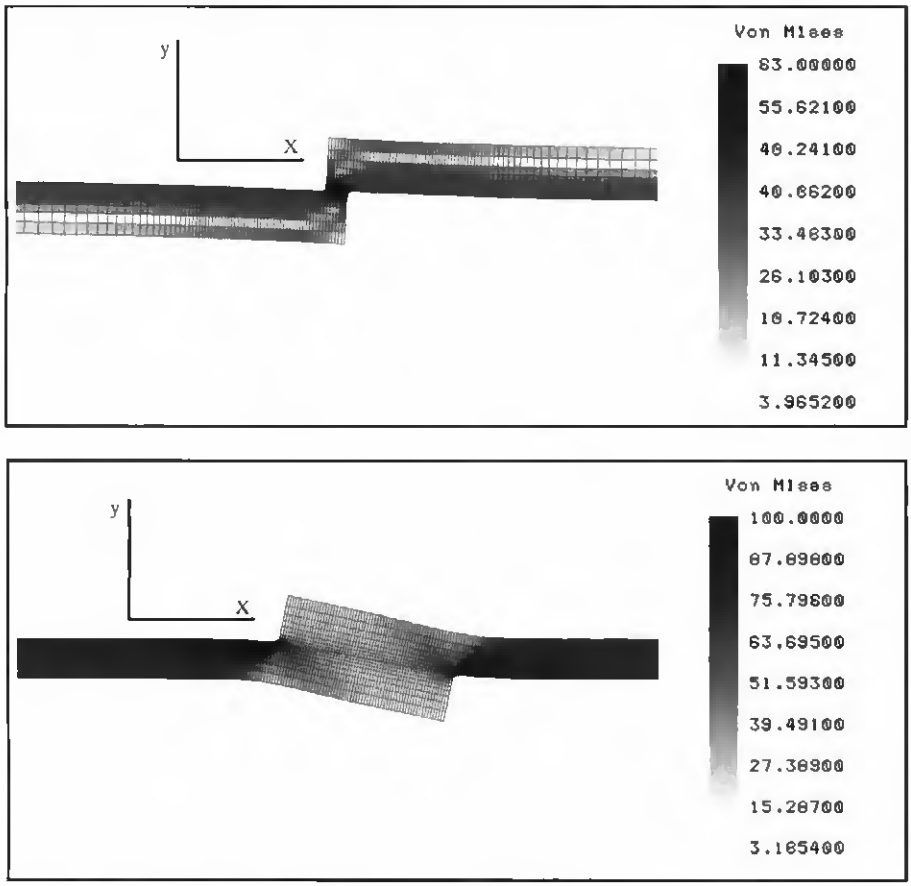


*Fig. 10 — Stress distribution in the lap braze joint at the failure load.*

the failures occurred in the filler metal. The elemental von Mises stress in the filler metal is used as the indication of the stress level in the filler metal. The question is: at what stress level will the filler metal fail? This is the fundamental question of the failure criterion of a brazed lap shear joint, which has no satisfactory answers.

A literature review indicates that von Mises stress was successfully utilized (Ref. 15) to demonstrate the decrease of the average shear stress in the lap joint with the increase of the overlap width, as shown in Fig. 1. Other studies (Ref. 16) considered the effects of the braze joint clearance, work hardening, and hydrostatic constraint on shear and tensile stress distribution, but did not discuss the braze joint failure criteria.

Our preliminary attempt was to use the ultimate tensile strength of the filler metal obtained from the tensile test as the failure criterion based on the single loading curve assumption (von Mises). The assumption is that the effective stress-strain curve coincides with the uniaxial tensile stress-strain curve, although the theory cannot predict the failure point. This attempt is apparently flawed, since the configuration of the filler metal in the brazed joint is so different from tensile test samples that the filler metal strength obtained in the two configurations will always be very different.

It is almost universally accepted that the ultimate failure strength of filler metal has to be tested in situ. The lap shear sample test is the most popular test. The lap shear test, however, determines the strength of the joint rather than filler metal strength — a property of the filler metal. The main reason for that is a nonuniform stress distribution in the filler metal of the lap shear joint. The trend of the SUS reduction with the increase of the lap width is not due to the fundamental property deterioration of the filler metal, but due to the joint configuration that causes the stress distribution to be less and less uniform.

The current analysis indicates that, for the short overlaps ($< 0.5T$), von Mises stress is fairly uniformly distributed within the filler metal, even far past the yielding point — Fig. 12. Thus, it is reasonable to think of the maximum von Mises stress observed in the filler metal with the overlap $\leq 0.5T$ as the shear strength of the filler metal. As the overlap width increases, the von Mises stress distribution becomes less and less uniform. The middle portion of the overlap contributes less and less to the overall load-carrying capacity of the joint, whereas the ends of the joint become "overloaded," i.e., von Mises stress exceeds maximum shear stress value of the filler metal (we define it as critical). The most striking feature shown in Fig. 12 is that at the failure loads, all von Mises stress distribution curves converge in the same point located approximately 5% of the overlap width away from the edge of the joint.

In other words, all lap shear test specimens failed when von Mises stress exceeded a certain critical value over some length that starts at the edge and extends into the joint. We can think of this length as a damage zone. The length of the damage zone is not constant but rather proportional to the overlap and equal to approximately 10% (5% from each end) of the overlap width. Consequently, we can define the failure of the ductile lap shear braze joints as follows: the ductile lap shear braze joint fails through the filler metal when the size of the damage zone exceeds certain critical value. Based on our observations, the size of the damage

zone for the stainless steel/silver combination is about 10% of the overlap width.

The concept of the damage zone is not new. In fact, it has been used quite extensively to define failure of adhesively bonded joints (Ref. 4). The authors, however, did not find any references where the damage zone concept was used to describe the failure of the braze joints. It is interesting to note that in the 1960s, when studying deformation of the lap joints with the help of photoelastic methods, the researchers were surprised to see the joint edges experienced loads far exceeding the yield point of the filler metal, while the overall load applied to the test specimens was still relatively small (Ref. 17)

It would be constructive to see if the damage zone concept can be applied to the experimental results reported by other researchers. To stay within the same family of base metal/ filler metal combinations, we selected the classic work of Bredzs and Miller (Ref. 18) to see if their test results can be correlated with our finite element analysis based on the 10% damage zone failure criterion. For this purpose, AWS BAg13 filler metal (Ag, Cu, and Zn alloy) was obtained and mechanically tested to generate a true stress-strain curve (Fig. 13), which is necessary for FEA-procedure. Indeed, the correlation between the experimental results and the FEA-predicted shear strength for the Bretz-Miller test specimens is quite good as shown in Fig. 14. Limited resources prevented the authors from comparing the damage zone based FEA results with other experimental data reported in the literature.

Although the strength of the filler metal in the lap shear braze joints is higher than the strength of the filler metals tested alone, it is realized that the von Mises stress cannot be as high as one would assume by looking at the edge regions in Fig. 12. Finite element analysis does not always give realistic values for the von Mises peak stress at the corners or edges. The von Mises curve usually capped around the discontinuity points using certain simplified values. For example, in the case of adhesive joints, the shear stress within the joint calculated using FEA procedure is capped by the shear strength of the adhesive (Ref. 4). In our case, however, it was decided to leave the von Mises stress plot as is, since it is not clear

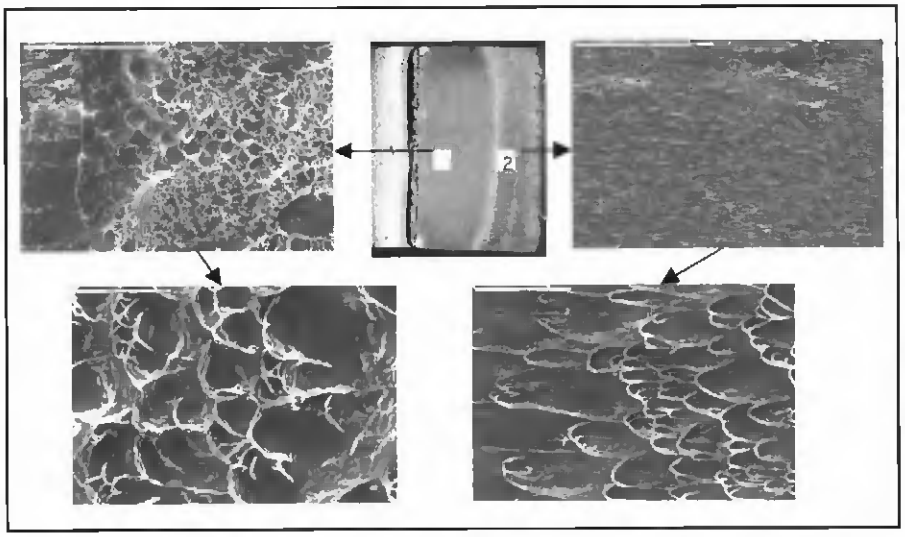


*Fig. 11 — Fracture surface of the electrolytically plated shear test specimen showing peel + shear (Region 1) and shear-dominated (Region 2) fracture modes. Shape of the dimples revealed on higher magnification images (300× and 2000×, progressively) confirms this observation.*

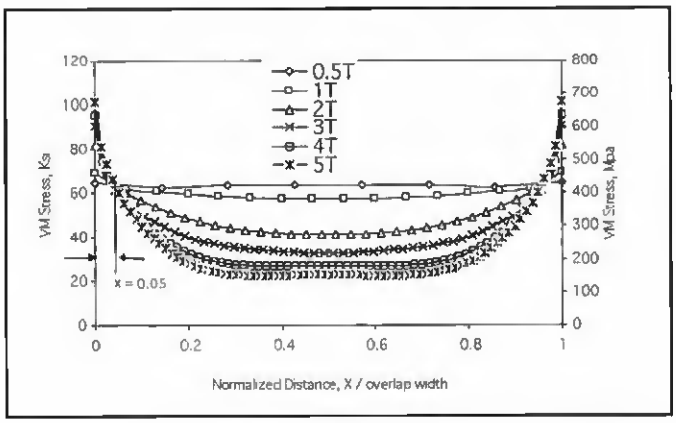


*Fig. 12 — Calculated values of the von Mises stress in the filler metal of the braze joints corresponding to the fracture of the shear test specimen. For convenience, the distance within the lap is given as a normalized value.*

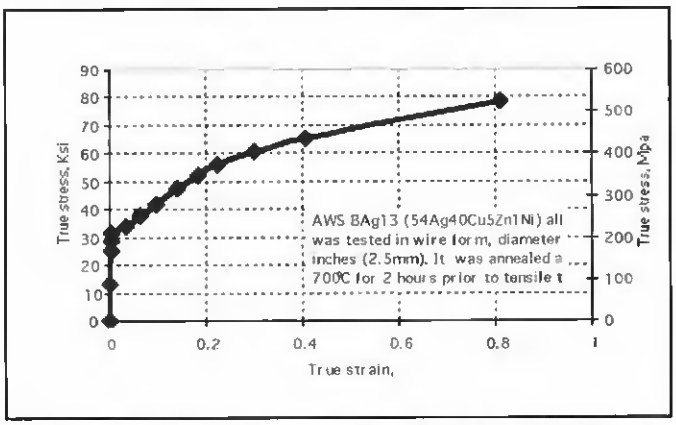


*Fig. 13 — True stress–strain curve generated for AWS BAg13 filler metal. Using these data, the damage zone based FEA was applied to compare our prediction with the results of Bredzs and Miller (Ref. 18.)*

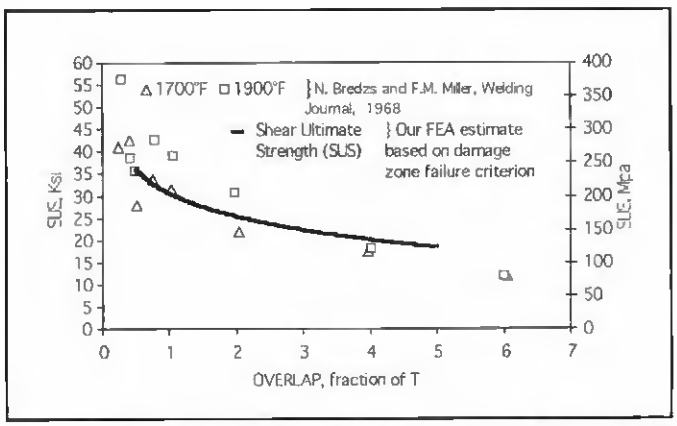


*Fig. 14 — Good agreement between the data by Bredzs and Miller (Ref. 18) for lap shear specimens brazed at two different temperatures and predicted SUS using a 10% damage zone.*

what value should be set as an upper limit for the von Mises stress in the lap shear braze joint damage zone. However, this investigation has demonstrated that, within the damage zone, the filler metal can be overloaded, but the joint does not fail until the size of the damage zone reaches a critical value.

## Conclusions

- It appears that for small overlaps (≤ 0.5T) stress distribution within the lap shear braze joint is uniform.
- The maximum von Mises stress calculated at failure in the 0.5T lap joint can be used as a critical or shear ultimate strength of the filler metal for the lap joint.
- Within the joint clearance sizes tested, 0.001–0.008 in. (25.4–203 mm), strength is not sensitive to clearance sizes.
- In the stainless steel lap shear joints brazed with silver metal, the failure occurs in the filler metal for overlaps up to 5T.
- It appears that the following damage zone criterion can be used: the lap shear braze joint fails if von Mises stress exceeds the critical value over 10% of the overlap area.
- The 10% damage zone observation checks well against other stainless steel/silver filler metal systems.

The authors would encourage other researchers to apply the damage zone failure criterion to their experimental data to see if this observation holds true for other base metal/filler metal combinations.

*Acknowledgments*

This effort was funded exclusively by the internal Goddard Space Flight Center flight programs. Specifically, the authors would like to thank Tom Venator and Kevin Grady (EOS AQUA), Robert Lilly and Martin Davis (GOES), and John Gagosian and Tony Comberiate (TDRSS) for their support and encouragement. Also greatly appreciated are numerous discussions on the subject matter with Robert Peaslee and his help in obtaining many valuable resources used in this work.

*References*

1. American Welding Society. 1963. C3.1-63, *Establishment of a standard test for brazed joints*, A committee report.

2. Johnson, W. S., ed. 1985. ASTM STP 876, *Delamination and Debonding of Materials*, American Society for Testing and Materials.

3. Johnson, W. S., ed. 1988. ASTM STP 981, *Adhesively Bonded Joints: Testing, Analysis and Design*. American Society for Testing and Materials.

4. Tong, L., and Steven, G. P. 1999. *Analysis and Design of Structural Bonded Joints*, Kluwer Academic Publishers.

5. Volkersen, O. 1938. Die niektraftverteiling in zugbeansprunchten mit konstanten laschenquerscritten. *Luftfahrforsch* 15: 41–47.

6. Military Specification MIL-B-007883C, 1986. *Brazing of Steels, Copper, Copper Alloys, Nickel Alloys, Aluminum and Aluminum Alloys*. Currently obsolete.

7. NASA. 1968. John F. Kennedy Space Flight Center Specification KSC-SPEC-Z-0005. *Specification for Brazing Steel, Copper, Aluminum, Nickel and Magnesium Alloys.*

8. ANSI/AWS C3.6:1999, *Specification for Furnace Brazing*. Miami, Fla.: American Welding Society.

9. ANSI/AWS C3.4:1999, *Specification for Torch Brazing*. Miami, Fla.: American Welding Society.

10. ANSI/AWS C3.5:1999, *Specification for Induction Brazing*. Miami, Fla.; American Welding Society.

11. ANSI/AWS C3.7:1999, *Specification for Aluminum Brazing*. Miami, Fla.: American Welding Society.

12. ANSI/AWS C3.2:2001, *Standard Method for Evaluating the Strength of Brazed Joints in Shear*. Miami, Fla.: American Welding Society.

13. Watkins, T., Jr. 1999. Private communications.

14. Dieter, G. E. 1976. *Mechanical Metallurgy*. McGraw-Hill, Inc.

15. Lugscheider, E., Reimann, H., and Knotek, O. 1977. Calculation of strength of single-lap shear specimen. *Welding Journal* 56(6): 189-s to192-s.

16. Shaw, C. W., Shepard, L. A., and Wulff, J. 1964. Plastic deformation of thin brazed joints in shear. *Transactions of ASM* 57: 94–109.

17. Peaslee, R. L. 2002. Private communications.

18. Bredzs, N., and Miller, F. 1968. Use of the AWS standard shear test method for evaluating brazing parameters. *Welding Journal* 47(11): 481-s to 496-s.